Cadherin activity is required for activity-induced spine remodeling

Ko Okamura,[1] Hidekazu Tanaka,[1] Yoshiki Yagita,[2,3] Yoshinaga Saeki,[4] Akihiko Taguchi,[5] Yasushi Hiraoka,[6] Ling-Hui Zeng,[1] David R Colman,[3] and Naomasa Miki[1]

[1]Department of Pharmacology and [2]Department of Internal Medicine, Osaka University Medical School, Suita, Osaka 565-0871 Japan
[3]The Montreal Neurological Institute, Montreal, Quebec H3A 2B4
[4]Neuro-Oncology Laboratory, Massachusetts General Hospital, Charlestown, MA 02114
[5]National Cardiovascular Center, Suita, Osaka 565-8565 Japan
[6]Kansai Advanced Research Center, National Institute of Information and Communications Technology, Kobe, Hyogo 651-2492 Japan

Neural activity induces the remodeling of pre- and postsynaptic membranes, which maintain their apposition through cell adhesion molecules. Among them, N-cadherin is redistributed, undergoes activity-dependent conformational changes, and is required for synaptic plasticity. Here, we show that depolarization induces the enlargement of the width of spine head, and that cadherin activity is essential for this synaptic rearrangement. Dendritic spines visualized with green fluorescent protein in hippocampal neurons showed an expansion by the activation of AMPA receptor, so that the synaptic apposition zone may be expanded. N-cadherin-venus fusion protein laterally dispersed along the expanding spine head. Overexpression of dominant-negative forms of N-cadherin resulted in the abrogation of the spine expansion. Inhibition of actin polymerization with cytochalasin D abolished the spine expansion. Together, our data suggest that cadherin-based adhesion machinery coupled with the actin-cytoskeleton is critical for the remodeling of synaptic apposition zone.

Introduction

Synaptic plasticity accompanies the structural remodeling of synapses. Recent advances in real-time visualization of neuronal contours in living tissues have shown that pre- and postsynaptic structures change their morphology in response to synaptic activity (Korkotian and Segal, 1999; Colicos et al., 2001; Hosokawa et al., 2003; Matsuzaki et al., 2004). Electron microscopic studies reveal a series of morphological changes with an enlargement and segmentation of the postsynaptic density, followed by the generation of multiple postsynaptic spines (Geinisman et al., 1991; Buchs and Muller, 1996; Toni et al., 1999; Ostroff et al., 2002). Of interest is that the zone of parallel apposition of pre- and postsynaptic membranes becomes enlarged by activity, giving rise to a broader area for chemical communication across the synaptic cleft (Buchs and Muller, 1996; Colicos et al., 2001). Furthermore, these structural modifications presumably depend on the remodeling of actin-cytoskeleton (Fischer et al., 2000; Colicos et al., 2001; Furuyashiki et al., 2002).

The CNS synapse is an adhesive junction comprising pre- and postsynaptic membranes, which are accompanied by the machinery for intercellular communication. Among certain families of adhesion proteins that have been suggested to be responsible for this adhesion, cadherins are likely to provide the adhesive force to maintain synaptic membranes in apposition (Yamagata et al., 1995; Fannon and Colman, 1996; Uchida et al., 1996; Benson and Tanaka, 1998; Inoue et al., 1998; Miskevich et al., 1998). Recent studies have shown that synaptic cadherins are involved in synaptic plasticity (Yamagata et al., 1999; Manabe et al., 2000). In particular, N-cadherin, which is enriched in hippocampal synapses (Benson and Tanaka, 1998), is required for the establishment of long-term potentiation (Tang et al., 1998; Bozdagi et al., 2000). Furthermore, N-cadherin rapidly redistributes after vigorous depolarization and acquires pronounced trypsin resistance, a property of stable cadherins engaged in adhesive interactions (Tanaka et al., 2000). The enhanced adhesiveness of N-cadherin is assisted by the recruitment of β-catenin to the activated synapse (Murase et al., 2002). The modification of N-cadherin with β-catenin is not dependent on new protein synthesis, probably providing the structural framework responsible for a rapid phase synaptic plasticity.

K. Okamura and H. Tanaka contributed equally to this work.

Correspondence to Hidekazu Tanaka: htanaka@pharma1.med.osaka-u.ac.jp

Abbreviations used in this paper: CCD, charge-coupled imaging device; DIV, day in vitro; SCCL, spine cotyloid curve length; W2A-cadherin, W2A mutant of N-cadherin.

The Journal of Cell Biology, Vol. 167, No. 5, December 6, 2004 961–972
http://www.jcb.org/cgi/doi/10.1083/jcb.200406030

N-cadherin is a member of the classical cadherin family, homophilic adhesion molecules with five extracellular subdomains separated from the cytoplasmic domain by a single transmembrane segment (Takeichi, 1990). The coupling of the cytoplasmic domain with the actin-cytoskeleton through catenins seems to be essential for full adhesive activity (Gumbiner and McCrea, 1993). Hence, cadherins provide the framework that links the cell–cell contact on the membrane surface to the cytoskeleton. However, it has not been directly studied whether cadherins are involved in the actin-mediated remodeling of synapses.

Here, we set out to the time-lapse analysis of GFP-visualized spines in order to understand the relationship between the morphological plasticity and the adhesive machinery linked to the actin-cytoskeleton. Activation of AMPA-glutamate receptor induces the lateral expansion of the spine surface that apposes the presynaptic membrane. The overexpression of a dominant negative form of N-cadherin abolishes the lateral spine expansion. Inhibition of actin-polymerization with cytochalasin D also blocks the spine expansion. This work suggests that the cooperation of the cadherin-actin complex is required for rearrangement of the adhesive surface of the synaptic junction, which could be at least in part responsible for the rapid phase of synaptic plasticity.

Results

Synaptic activity induces the lateral expansion of spine head

To study the morphological plasticity of postsynaptic spine, we performed time-lapse video imaging of cultured hippocampal neurons visualized with GFP. Rat neurons isolated from embryonic day 18 embryos were transfected with the cDNA for *gfp* on the sixth day in vitro (DIV), and subjected to time-lapse charge-coupled imaging device (CCD) imaging on 18–22 DIV, when dendrites display numerous mature spines (Fig. 1 A). The GFP diffusely distributed through cytoplasm, and labeled the contour of dendritic protrusions. At this stage, 49% of the protrusions appeared on dendritic surface showed cotyloid appearance (Fig. 1 B, closed arrow), and 17% showed flat-apex mushroom appearance (closed arrowhead; Table I). These two types are the ones classically recognized as typical mature spines with bulged heads connected to the dendritic shaft with short necks. There were also thin spines with long necks (Fig. 1 B, open arrow; 12%), and filopodia (Fig. 1 B, open arrowhead; 22%; Table I). The cotyloid spine top was closely apposed to a presynaptic terminus labeled by synaptophysin, suggesting that this surface forms an adhesive contact with the presynaptic membrane (Fig. 1 C).

We treated neurons with high K^+ (31 mM) for 2 min, and then observed them for a further 60 min to analyze the morphological plasticity of spines (Fig. 1 D). During membrane depolarization, the spines became round within a few seconds (Fig. 1 D, depol) as reported previously (Fischer et al., 2000). Immediately after repolarization, the shape of the spines was recovered (Fig. 1 D, recovery 5′). Within 15 min of the recovery, the lateral extent of the spines became enlarged compared with the resting state (Fig. 1 D, recovery 15′). This enlargement peaked at 15–30 min after the stimulation, and spines remained slightly enlarged at 60 min (Fig. 1 D).

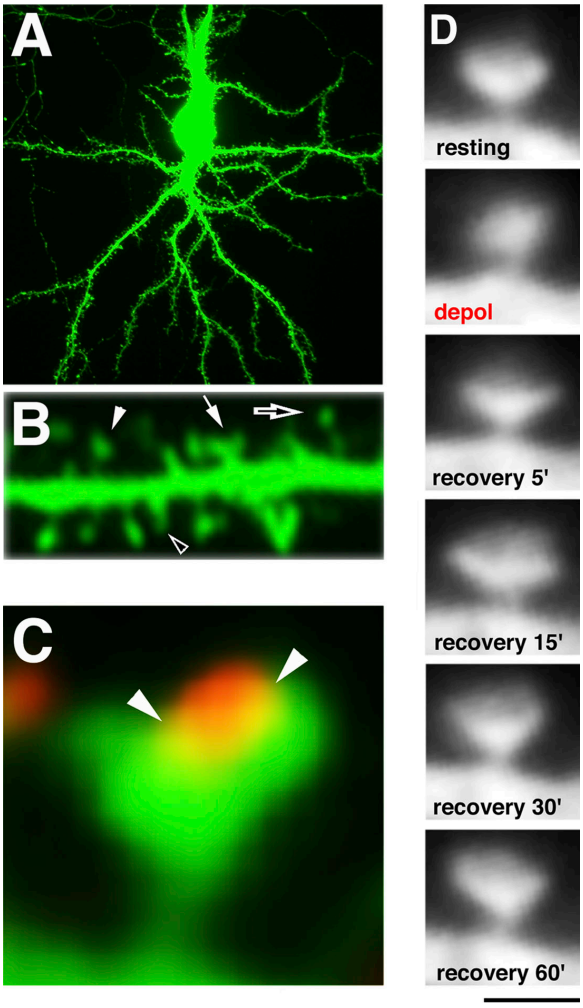

Figure 1. **Depolarization induces the lateral expansion of spine head.** Hippocampal neurons were transfected with *gfp* and subjected to CCD imaging on 18–22 DIV. (A) GFP uniformly labels the neuronal contour. (B) Closer magnification of a GFP-filled dendrite. Closed arrow, cotyloid spine; closed arrowhead, flat apex spine; open arrow, thin spine; open arrowhead, filopodium (Table I; Fig. 7 C). (C) The GFP-filled neurons were immunolabeled with synaptophysin (red). The presynaptic terminal labeled by synaptophysin attaches to the cotyloid face on the apex of the spine. Arrowheads indicate putative synaptic cleft. (D) GFP-labeled neurons were transiently treated with high K^+ (31 mM) for 2 min, and recovered for 60 min in normal K^+ solution, while images were taken serially. The spine rounded up during the depolarization (2 min), and then displayed cotyloid shape again when the stimulation was halted (recovery 5′). The lateral size of the spine became larger than in the original at 15 min after the stimulation (recovery 15′), and it lasted at least for 60 min (recovery 60′). Bar: (A) 60.00 μm; (B) 5.00 μm; (C) 1.00 μm; (D) 1.25 μm.

To quantify this spine enlargement, we took advantage of a confocal microscope (Fig. 2). The three dimensional information of the spine of interest was analyzed by optical section (*z*-series) images collected at 0.2 μm focus intervals. The profile of the *z*-stack images was sufficient to obtain an unambiguous spine profile (Fig. 2 A). The width of spine heads was measured on the spine profile being thresholded at half maximal fluorescence intensity (Fig. 2 B). The maximum spine width was determined by laying the axis as to run across the widest point of the spine head (Fig. 2 B, gray line). The spine width changed from 1.18 ± 0.0490 μm to 1.36 ± 0.0620 μm (Fig. 2 C; mean ± SEM).

Table I. **Shape of protrusions in neurons transfected with *N-cadherin* mutants**

	gfp	*N-cadherin*	*W2A-cadherin*	*NcadΔE*
	***n* = 202 (12)**	***n* = 343 (20)**	***n* = 294 (18)**	***n* = 322 (17)**
Cotyloid spine (**C-1)	49%	57%	16%	14%
Flat apex spine (**C-2)	17%	17%	32%	30%
Thin spine (**C-3)	12%	10%	13%	12%
Filopodia (**C-4)	22%	16%	39%	44%

Neurons were doubly transfected with *gfp* and either *N-cadherin, W2A-cadherin, NcadΔE*, or *mock* on 6 DIV. On 21 DIV, the type of each protrusion sprouted on the 20-μm segment between 20 and 40 μm from the proximal origin of the main (thickest) dendrite was judged by shape. Spine (C-1, -2, -3) was judged by the bulging head connected to the dendritic shaft via thin neck. The spine whose width was equal to or more than half the size of its length was judged as standard mushroom spine. Standard mushroom spines were divided into the one with cotyloid apex (C-1) and one with flat apex (C-2). The spine whose width was smaller than half the size of its length was judged as thin spine (C-3).
*No. of protrusions subjected to evaluation, with No. of neurons in parentheses. The No. of experiments was equal to the No. of neurons.
**Typical examples are shown in Fig. 7 C.

Recording *z*-stack images resulted in blurring due to the rapid spine motility (Fischer et al., 1998) during the data collection through *z*-series. In addition, typical cotyloid and mushroom spine profiles were largely masked by stacking the multiple images at different z positions. In this work, therefore, further analyses were performed on the single optical section that passes through the maximum spine diameter among *z*-series images. The chosen optical section showed clearer cotyloid shape with similar size to the z-stack image (Fig. 2 D). The spine width measured on the thresholded single optical section changed from 1.13 ± 0.0500 μm to 1.34 ± 0.0570 μm (Fig. 2 E). Together, the data suggest that the lateral size of spine enlarges in response to membrane depolarization.

Although the confocal technology enables us to avoid out-of-focus image blurring, it takes at least tens of seconds to collect data of the area that includes several spines, while the spine changes its shape within several seconds (Fischer et al., 1998). To obtain time-lapse images rapidly enough, we collected only a single focus image at each time point with 6-s intervals by the use of a CCD; these experiments confirmed the rapid spine motility (Fig. 3 A). We measured the dimensions of spines from these single-focus images. Measurements of the (a) width, (b) length, and (c) curve of the apex of the spine (spine cotyloid curve length [SCCL]) were performed on thresholded images at half maximal fluorescence intensity (Fig. 3 C). A possible drawback of this procedure, however, is a limited resolution. Therefore, we obtained optical section images of the GFP-filled spines in fixed neurons, and compared undeconvoluted images with deconvoluted ones (Fig. 3 B). In spite of the relatively low resolution of the undeconvoluted images, the dimensions measured on these undeconvoluted images were very well correlated with those measured on the deconvoluted images (Fig. 3 D). For further accuracy, we averaged the values obtained from 21 time series with 6-s intervals for each time window of 2 min.

Measurements performed on the CCD image revealed that the width of individual spine after depolarization became larger than the one in resting condition, whereas the spine length remained at the basal level (Fig. 3, E and H). The mean spine length being 2.16 ± 0.137 μm at rest remained 2.21 ± 0.138 μm. The mean spine width changed from 1.01 ± 0.0436 μm to 1.14 ± 0.0455 μm. The observation was consistent with the data obtained by the use of a confocal microscope (Fig. 2).

In addition to the spines with laterally broad heads, there were spines with their apexes curved deeply (Fig. 3 F). This type of spine did not show lateral expansion, but extended the both ends of the cotyloid curves longitudinally. However, this

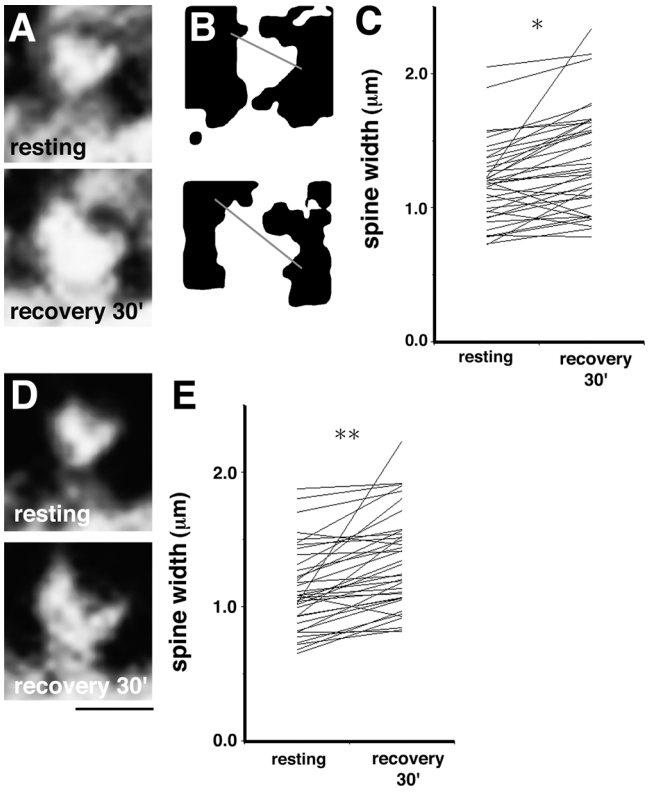

Figure 2. **Evaluation of spine broadening by confocal microscopy.** *Z*-series profiles of GFP-filled spine were collected at 0.2-μm focus intervals by using a confocal microscope at resting state and 30 min after stimulation (high K^+ for 2 min). (A) *Z*-stack image represents enlargement of the lateral diameter of spine. (B) *Z*-stack image was thresholded at half maximal fluorescence intensity. An axis was laid as to run across the widest point of spine head (gray line). (C) The spine width measured at the widest point before and 30 min after depolarization is plotted. *$P < 0.00002$. (D) The single optical section that passes through the maximum spine diameter among z-series images. Note that the maximal optical section showed clear cotyloid shape with similar lateral size to the z-stack image. (E) The spine width measured on the maximal optical section before and 30 min after depolarization is plotted. **$P < 0.000003$. The measurements of 38 spines of four neurons (dendrites) were collected from four independent experiments (C and E). Bar, 1.25 μm.

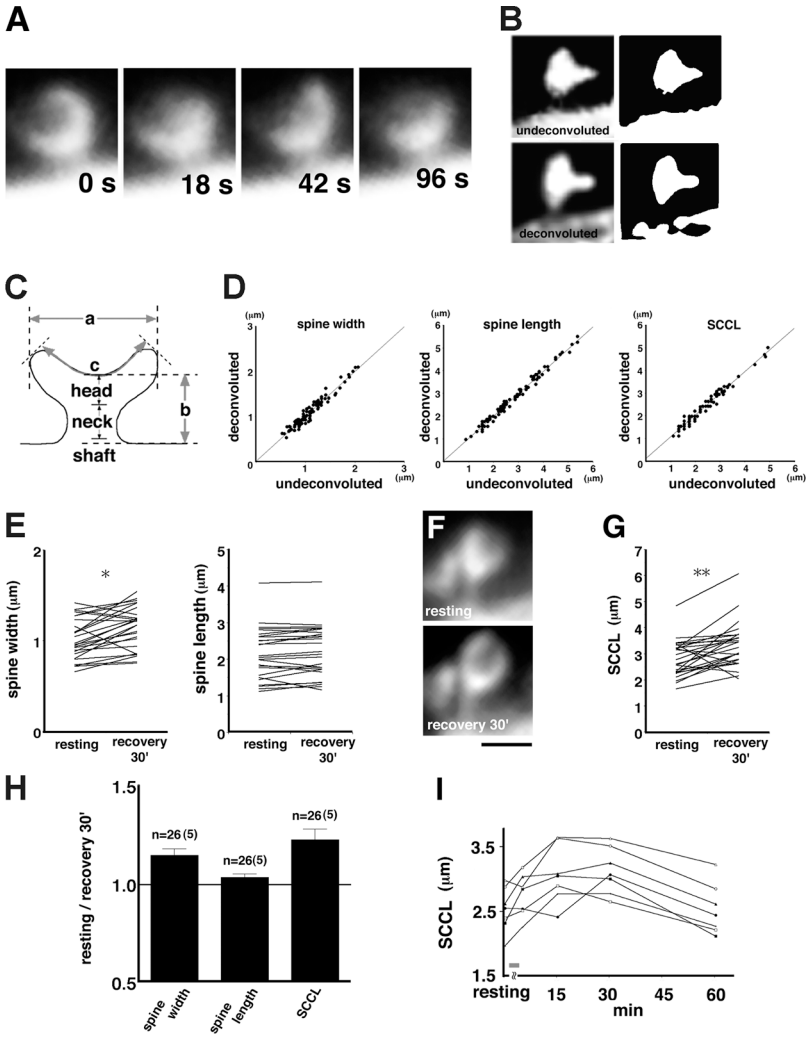

Figure 3. **Evaluation of spine remodeling on deconvolution and conventional microscopy.** (A) Capturing CCD images at short intervals demonstrate rapid movement of a spine. (B) Comparison of a raw CCD image (top) with a deconvoluted image (bottom) of spine. (Right) Thresholded images at half maximal fluorescence intensity. (C) Discernment of the (a) spine width, (b) spine length, and (c) SCCL. (D) Dimensions measured on raw CCD images were plotted against those measured on deconvoluted images. $R^2 = 0.944$ (width), $R^2 = 0.986$ (length), $R^2 = 0.965$ (SCCL). (E) The spine width (left) and length (right) of each spine before and 30 min after depolarization are plotted. $^*P < 0.001$. (F) A spine with deeply curved apex. Note that the apex curve extends longitudinally. (G) SCCL of each spine before and 30 min after depolarization are plotted. $^{**}P < 0.0006$. (H) The ratios between resting spine parameters and stimulated (30 min) spine parameters are shown (mean ± SEM). (I) Temporal profiles of the SCCL of each spine. The SCCL of each spine peaks between 15 and 30 min after the stimulation. The measurements of 26 spines of five neurons (dendrites) were collected from five independent experiments (E, G, and H). Bar: (A) 1.52 μm; (B) 1.40 μm; (F) 1.50 μm.

type of spine also appeared to broaden the adhesive contact surface, where the spine apex is apposed to the presynaptic membrane (Fig. 1 C). Therefore, it seems reasonable to measure the SCCL in order to include the remodeling of the deep cotyloid spines (Fig. 3 C). As expected, the change in SCCL was found to be more prominent than one in simple spine width (Fig. 3 G). The mean SCCL changed from 2.80 ± 0.136 to 3.38 ± 0.168 μm. The mean SCCL at 30 min after the depolarization became 1.22 ± 0.0527 times larger than the resting state (Fig. 3 H). The temporal profiles of the SCCL of individual spines differ with each other, but the enlargement usually peaked at 15 or 30 min after the stimulation (Fig. 3 I). The data support the hypothesis that strong synaptic inputs accelerate synaptic efficacy, which may accompany the expanded area size for the trans-synaptic communication (Buchs and Muller, 1996; Tanaka et al., 2000; Colicos et al., 2001).

The AMPA receptor–mediated pathway is responsible for the spine broadening

Dendritic spines comprise an excitatory postsynaptic structure equipped with glutamate receptors. To see if the lateral spine enlargement is coupled with excitatory synaptic functions, we tried to identify the pathway responsible for the phenomenon. In the presence of an AMPA receptor antagonist CNQX (100 μM), neither spine shrinkage during depolarization, nor spine enlargement after recovery occurred (Fig. 4). The mean SCCL being 3.41 ± 0.175 μm at rest remained 3.38 ± 0.160 μm in 30 min of recovery. In contrast, an NMDA receptor antagonist APV (100 μM) did not strongly affect these responses of the spines (Fig. 4). The mean SCCL changed from 2.63 ± 0.103 μm to 3.08 ± 0.112 μm in 30 min of recovery. The data suggest that the broadening of spine head is under the influence of AMPA-type glutamate receptor activation. The observation is consistent with the hypothesis that the rapid rearrangement of the synaptic adhesion zone might be related to the rapid phase of synaptic plasticity.

N-cadherin is redistributed along the expanding surface of spine head

N-cadherin may be important in the maintenance of excitatory synapses in cultured hippocampal neurons (Benson and Tanaka, 1998). In addition, N-cadherin is involved in the plasticity and the morphogenesis of hippocampal synapses (Tang et al., 1998; Bozdagi et al., 2000; Togashi et al., 2002; Bamji et al., 2003; Abe et al., 2004). Indeed, N-cadherin immunoreactivity has been shown to disperse along with the expansion of the synaptic cleft upon massive synaptic stimulation (Tanaka et al., 2000).

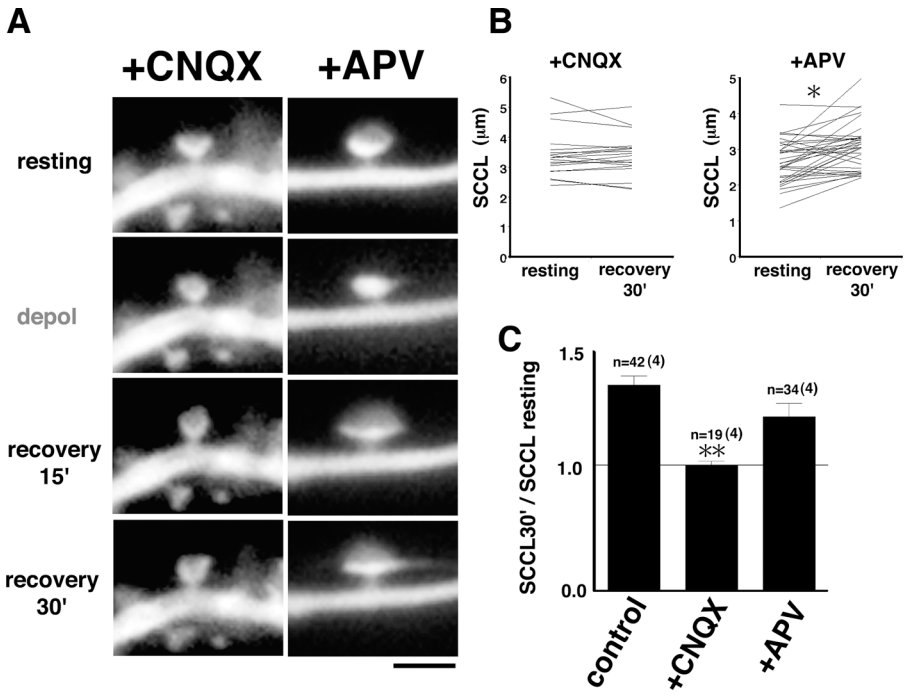

Figure 4. **AMPA receptor activation is involved in the spine expansion.** (A) Time-lapse imaging of GFP-filled spines was performed in the presence of glutamate receptor antagonist, CNQX or APV. CNQX but not APV blocked the depolarization-induced spine expansion. (B) The SCCL of each spine before and 30 min after depolarization is plotted. *P < 0.003. (C) The ratios between resting SCCL and stimulated (30 min) SCCL are shown (mean ± SEM). **P < 0.05 to control and +APV. The measurements of 42 (control), 19 (CNQX), and 34 (APV) spines of four neurons (dendrites) were collected from four independent experiments. Bar, 2.50 μm.

To gain insight into the involvement of N-cadherin in the activity-induced enlargement of the spine head, we pursued the redistribution of N-cadherin by expressing recombinant N-cadherin fused with the Venus fluorescent protein, a variant of GFP (Fig. 5 A; Nagai et al., 2002). Although Venus was ligated adjacent to the catenin-binding domain of N-cadherin, N-cadherin-venus normally bound to β-catenin and exhibited homophilic adhesive activity on transfected L929 cells (unpublished data). N-cadherin-venus was distributed widely throughout the spine head, whereas PSD-95, a postsynaptic density marker protein, was often restricted to the center of the spine head (Fig. 5 B). The distribution of N-cadherin-venus well fitted in with the distribution of intrinsic N-cadherin as examined by immunostaining (Fig. 5 C). N-cadherin-venus was redistributed along the laterally moving spine head in resting state (Fig. 5 D). Upon depolarization, N-cadherin-venus showed lateral dispersion along the expanding spine head (Fig. 5, E and F). The lateral extent of spinal N-cadherin changed from 3.23 ± 0.222 μm to 3.60 ± 0.274 μm in 30 min of recovery. Thus, N-cadherin seems to be redistributed in accordance with the broadening of the synaptic apposition zone.

It is reported that the N-cadherin immunoreactivity disperses during depolarization, but it reconsolidates to form synaptic puncta again after 15 min of recovery phase (Tanaka et al., 2000). Consistent with this notion, immunoreactive N-cadherin puncta before and 30 min after depolarization showed no obvious difference apparently. To our surprise, however, the gross measurement of the area size of N-cadherin puncta revealed that the puncta became enlarged slightly (Fig. 5 G). This change might reflect the lateral dispersion of endogenous N-cadherin along the broadening of the spine head.

To rule out the possible artifact by the overexpression of N-cadherin in the experiments above, we examined the effect of overexpression of N-cadherin on the change in spine shape. We cotransfected *N-cadherin* and *gfp* cDNAs into cultured neurons, and confirmed that the green neurons coexpressed abundant recombinant N-cadherin by immunostaining retrospectively (Fig. 6 A). 57% of the dendritic protrusions displayed typical cotyloid spine, whereas only 16% were filopodia (Table I). The data suggest that overexpression of N-cadherin increases the ratio of mature spine and decrease the ratio of filopodia. However, the total number, and the mean length of the protrusions were not changed by the overexpression of N-cadherin (Fig. 7 D; Table II). The morphological responses to membrane depolarization were essentially the same as in the control neurons; the spines rounded up and halted during the depolarization, and became enlarged after the repolarization (Fig. 6 B). The mean SCCL changed from 3.08 ± 0.0975 μm to 4.00 ± 0.134 μm in 30 min of recovery (Fig. 6 C). The extent of the spine enlargement was similar to that in control neurons (1.32× enlargement of SCCL, SEM = 0.0359; Fig. 7 J).

Cadherin activity is required for the activity-induced spine head expansion

To examine if cadherin function is essential for the activity-induced spine enlargement, we took advantage of the W2A mutant of N-cadherin (W2A-cadherin), a point mutant that lacks adhesive activity (Tamura et al., 1998). The overexpression of W2A-cadherin suppressed the adhesive function of N-cadherin as examined by cell aggregation assays (Fig. 7 A). The number of dendritic protrusions on the neurons overexpressing W2A-cadherin was equal to the spine number on the control neurons (Table II). 16% of these spines on the W2A-transfected neurons remained in normal cotyloid shape (Fig. 7 C-1; Table I). 32% of spines appeared largely normal with their heads still identifiable as the bulging end, but their apexes were flat without cotyloid curve (Fig. 7 C-2; Table I). This type of spine was occasionally accompanied by transient protrusions on its apex (see

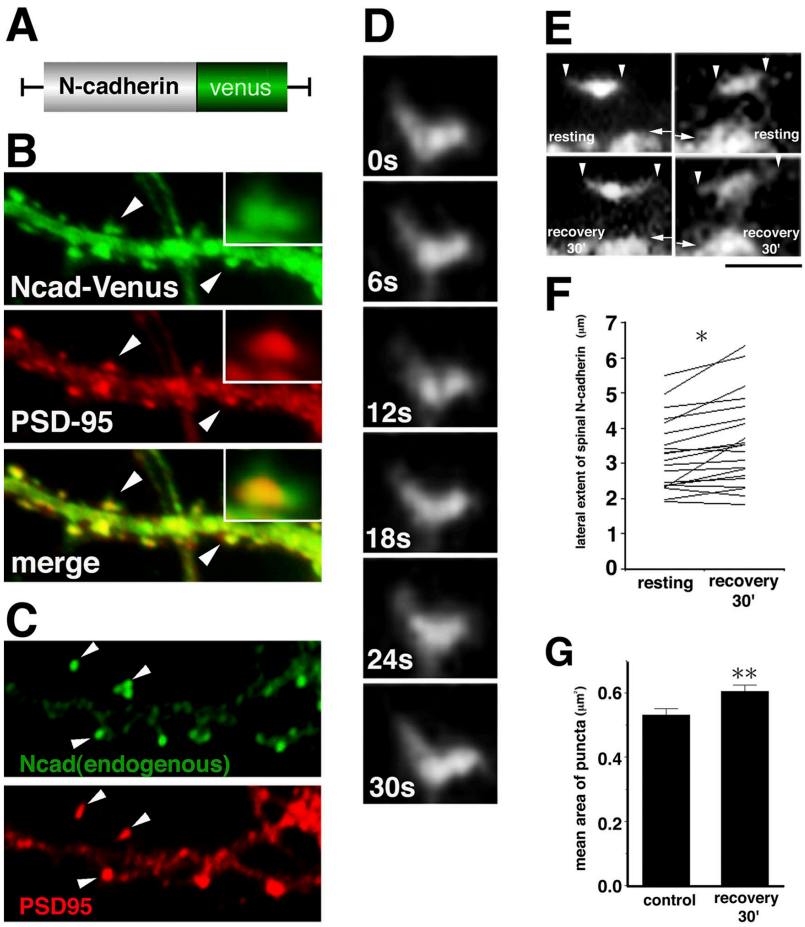

Figure 5. **N-cadherin was redistributed along the expanding spine head.** Neurons were transfected with *N-cadherin-venus* fusion cDNA and subjected to time-lapse imaging. (A) Diagram shows the construction of *N-cadherin-venus*. (B) Immunostaining of a *N-cadherin-venus* transfected neuron. N-cadherin-venus is accumulated in dendritic spines positive with PSD-95 (arrowheads). Inset, closer magnification of a spine. (C) Immunostaining for endogenous N-cadherin and PSD-95. Arrowheads indicate spines. (D) Movements of N-cadherin-venus on spine head at rest. Note that the fluorescent signal shifts laterally. (E) N-cadherin-venus expressed on the apical surfaces of the spines before (top) and 30 min after (bottom) the depolarization. N-cadherin-venus dispersed along the expanding spine head. Arrowheads indicate lateral extents of spine heads; arrows indicate an edge of a dendritic shaft. (F) The lateral N-cadherin extent of each spine before and 30 min after depolarization is plotted. The length of the curve on the top of the N-cadherin-venus positive region, which presumably corresponds to SCCL was measured. The measurements of 21 spines of nine neurons (dendrites) were collected from nine independent experiments. *$P < 0.001$. (G) The graph shows the area size of N-cadherin immunoreactive puncta (mean ± SEM) before and 30 min after stimulation. The data were collected from four independent experiments. **$P < 0.01$. Bar: (B) 10.00 μm; (B, inset) 3.00 μm; (C) 6.00 μm; (D) 1.67 μm; (E) 1.30 μm.

Fig. 8 D). 13% showed normally bulged spine head, but with elongated neck (Fig. 7 C-3; Table I). The other 39% showed filopodia-like elongated shape (Fig. 7, C-4; Table I). The mean length of all these four types of protrusions were measured and found to be longer than the normal neurons (Fig. 7 D). The data were consistent with the previous report that has shown the spine elongation induced by another dominant negative form of N-cadherin or αN-catenin mutation (Togashi et al., 2002; Abe et al., 2004). We also confirmed this by using another dominant negative form, NcadΔE that totally lacks the extracellular domain (Fig. 7 D; Kintner, 1992). In spite of such morphological anomaly, the apex of the majority of these former three types of protrusions (C-1, C-2, C-3) were positive with PSD-95 and apposed to a presynaptic terminus (Fig. 7 E), suggesting that the adhesion of pre- and postsynaptic membranes were maintained.

We then focused our analyses on the normal shape (C-1) and flat apex (C-2) spines, and pursued the morphological plasticity during and after neural stimulation. Depolarization of the *W2A-cadherin* transfected neurons resulted in rounding up and freezing as observed in control neurons (Fig. 7 F). However, there was no lateral enlargement observed during the recovery phase (Fig. 7 F). The lateral size of spines became rather smaller than in the resting state. The spine width changed from 1.17 ± 0.0374 μm to 1.02 ± 0.0377 μm in 30 min of recovery (Fig. 7 G). The observation was confirmed by the analysis using a confocal microscope; the spine width changed from 1.36 ± 0.076 μm to 1.12 ± 0.049 μm in 30 min of recovery (Fig. 7, H and I). Moreover, rapid frame time-lapse analyses enabled us to distinguish the core portion of C-2 type spines from the additional protrusions that move very quickly and randomly and that disappear shortly (see Fig. 8 D). Thus, we ruled out transient protrusions, and could determine the spine apex curve for the measurement. The SCCL changed from 3.16 ± 0.146 μm to 2.52 ± 0.136 μm in 30 min of recovery (Fig. 7, G and J). All these observations were confirmed by using another dominant negative cadherin construct, *NcadΔE* (Fig. 7, D and J; Tables I and II). The data suggest that cadherin activity is necessary for the lateral expansion of spine in response to synaptic activity as well as for the maintenance of the spine shape.

By the overexpression of W2A-cadherin, the distribution of AMPA receptor as marked by GluR2/3 immunoreactivity remained normal accumulating on spines (Fig. 7 K). Therefore, the synaptic input and the subsequent signal transduction through the AMPA receptor may not be disturbed by W2A-cadherin. Together, the abolishment of the activity-induced spine expansion with W2A-cadherin is unlikely to be a secondary event due to the abrogation of AMPA receptors.

Activity-induced spine head expansion is dependent on actin polymerization

The rapid motility of spines is dependent on actin polymerization (Fischer et al., 1998). In addition, cadherin-based adhesion

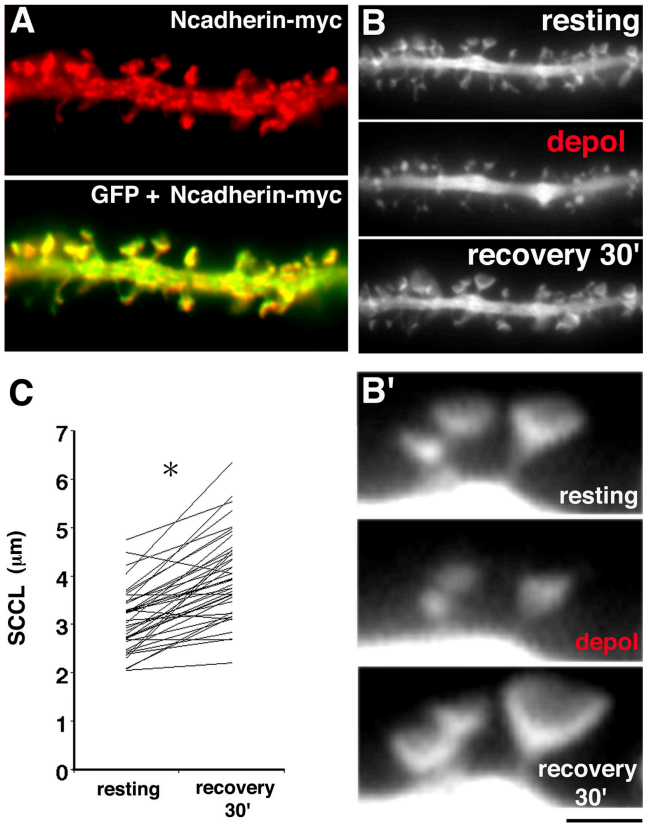

Figure 6. **Remodeling of spine in *N-cadherin* transfected neuron.** Neurons were doubly transfected with *gfp* and *N-cadherin-myc* and subjected to time-lapse imaging. (A) Retrospective immunostaining with anti-myc antibody confirms that the green neuron overexpresses N-cadherin-myc. N-cadherin-myc is accumulated in spines. (B) Time-lapse imaging of the *N-cadherin-myc* transfected neuron before, during and after a 2-min depolarization. Spines display rounding up during the depolarization, and the lateral enlargement during the recovery phase. B′ depict magnified images. (C) The SCCL of each spine before and 30 min after depolarization is plotted. The measurements of 42 spines of four neurons (dendrites) were collected from four independent experiments. *$P < 0.0000004$. Bar: (A) 5.00 μm; (B) 7.33 μm; (B′) 2.00 μm.

is dependent on linkage to the actin-cytoskeleton, bridged by β- and α-catenins (Gumbiner and McCrea, 1993). Therefore, we examined if the cadherin-dependent spine remodeling is associated with the actin polymerization. Low concentration of cytochalasin D arrests spine motility without significant depolymerization of preexisting actin fibers (Fischer et al., 1998). In the presence of 40 nM cytochalasin D, spines showed rounding up during depolarization, suggesting that the phenomenon is not dependent on actin polymerization (Fig. 8 A). In contrast, no enlargement of the spines was observed during the recovery phase in the presence of cytochalasin D (Fig. 8, A–C). The mean SCCL being 3.14 ± 0.102 μm at rest remained at 3.33 ± 0.137 μm in 30 min of recovery in the presence of cytochalasin D. The data indicate that the activity-induced expansion of spines is dependent on the remodeling of the actin-cytoskeleton, as well as its surface partner, the cadherins.

Cadherin and actin-cytoskeleton are required for the maintenance of spine structure

During the time-lapse observation of the W2A-cadherin overexpressed neurons, we realized multiple filopodia-like structures protruding from the top of the spines in response to depolarization (Fig. 8 D, arrows). These transient protrusions were occasionally found in resting neurons, too. The protrusions appeared at various time points, during and after completion of the depolarization period. The protrusions then fused with each other within 15 min while randomly moving in various directions (Fig. 8 D, recovery 15′-30′). It is expected that the link between the intrinsic cadherin and the cytoskeletal elements may be disconnected in the W2A-cadherin overexpressed neurons.

Therefore, we asked whether the spine shape is dependent on F-actin itself. To address this, F-actin was depolymerized using the G-actin binding drug latrunculin B, and its effect on spines was assessed. Addition of 5 μM latrunculin B, which results in a progressive loss of F-actin (Zhang and Benson, 2001), resulted in a rough spine head with random protrusions (Fig. 8 E, arrowheads). Together, the data suggest that synaptic stimulation drives the polymerization of actin and the remodeling of cytoskeleton, which in turn results in the random and transient protrusion of filopodia-like structures, as the actin-cytoskeleton is disconnected from the cadherin-based adhesion apparatus. On the other hand, this driving force might result in the normal expansion of the synaptic adhesion zone, if there are enough cadherin molecules to link with the activity-driven actin-cytoskeleton in synaptic membranes.

Change in diffusion rate of GFP does not affect spine profile

There is possibility that the change in shape of GFP-filled spine is interfered by the alteration of the diffusion rate of soluble GFP. The change in molecular diffusion rate in response to synaptic activity has been observed in the case with the membrane bound form of the GFP (Richards et al., 2004). To assess the extent of the possible influence due to the diffusion rates of GFP, we have performed FRAP experiments in GFP-filled spines under various conditions (Fig. 9). In either condition, the diffusion of soluble GFP was so rapid that we observed subsecond recovery curves as reported previously (Majewska et al.,

Table II. **No. of protrusions in neurons transfected with *N-cadherin* mutants**

	gfp	*N-cadherin*	*W2A-cadherin*	*NcadΔE*
Protrusion No./20 μm dendrite	18.5 ± 0.734 *n = 19 (19)	16.6 ± 0.725 *n = 19 (19)	17.6 ± 1.03 *n = 15 (15)	18.7 ± 1.15 *n = 15 (15)

Neurons were doubly transfected with *gfp* and either *N-cadherin, W2A-cadherin, NcadΔE,* or *mock* on 6 DIV. On 21 DIV, any protrusion sprouted on the 20-μm segment between 20 and 40 μm from the proximal origin of the main (thickest) dendrite was counted. Mean ± SEM are shown.
*No. of neurons subjected to counting, with No. of experiments in parentheses.

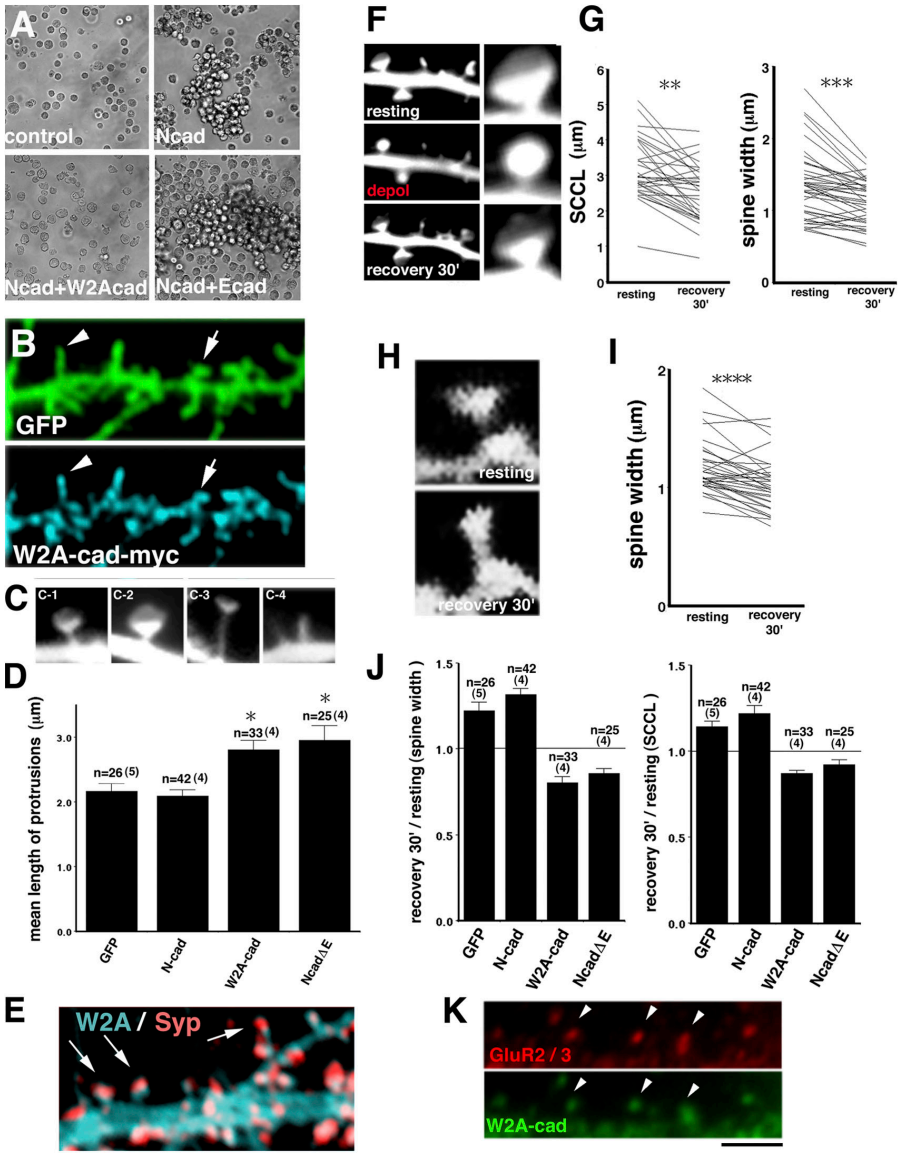

Figure 7. **W2A-cadherin abrogates the spine head expansion.** (A) Aggregation of L929 cells stably expressing N-cadherin (Ncad) and/or W2A-cadherin (W2Acad). The homophilic adhesiveness of N-cadherin yielded large cell aggregates. Co-expression of W2A-cadherin suppressed the adhesiveness of N-cadherin (Ncad+W2Acad). E-cadherin does not change the N-cadherin adhesiveness (Ncad+Ecad). (B) The shape of spines in the *W2A-cadherin* transfected neurons fixed with PFA. Green, GFP; blue, W2A-cadherin. A subpopulation of spines display extended morphology (arrowheads) as well as normal shape (arrows). (C) Examples of typical protrusion morphologies. C-1, cotyloid spine; C-2, flat apex spine; C-3, thin spine; C-4, filopodia. (D) Mean lengths of the protrusions are shown. *$P < 0.01$ to GFP. (E) Double immunostaining of the *W2A-cadherin* transfected neurons with synaptophysin. The spines are apposed with synaptophysin puncta (red, arrows). (F) Time-lapse series of a *W2A-cadherin* transfected neuron. Depolarization induces the rounding up and the freezing (depol) as observed in control neurons. There is no enlargement of the lateral spine size during the recovery phase (recovery 30′). (G) The SCCL (left) and spine width (right) before and 30 min after depolarization are plotted. **$P < 0.0002$; ***$P < 0.00002$. (H) Change in spine shape was detected with confocal microscopy. (I) The spine widths measured on confocal images are plotted. ****$P < 0.000003$. (J) The graphs show changes in spine width (left) and SCCL (right) in 30 min after depolarization. Neurons were transfected with *mock* (*GFP*), *N-cadherin* (*N-cad*), *W2A-cadherin* (*W2A-cad*), and *NcadΔE*. (K) Immunostaining of the neuron transfected with *W2A-cadherin*. GluR2/3 immunoreactivity normally localized in spines (arrowheads). The data were collected from four to five neurons (dendrites) in four to five independent experiments for each group (D, G, I, and J). The data are shown as mean ± SEM (D and J). Bar: (A) 125 μm; (B) 5.00 μm; (C) 1.56 μm; (E) 5.00 μm; (F, left) 4.50 μm; (F, right) 1.50 μm; (H) 1.50 μm; (K) 3.71 μm.

2000). There was no detectable difference in the FRAP of cadherin-inactivated neurons (Fig. 9 B). Although there was some delay in recovery with the addition of cytochalasin D, submaximal recovery was achieved within 1 s (Fig. 9 C). Therefore, the change in spine size may not be interfered by the diffusion rate of GFP. Moreover, we observed rapid spine motility both before and after depolarization. This suggests that the GFP diffusion was rapid enough to fill the moving spine in this time course. Therefore, the shape change of GFP-filled spine in control, N-cadherin inactivated, and cytochalasin D–treated neurons likely reflect the actual change in spine shape.

Discussion

Synaptic transmission in CNS is a chemical event mediated by neurotransmitters released from the presynaptic terminal, and their receptors and associated signaling molecules that exist at the postsynaptic membrane. According to this physiological concept, studies on synaptic plasticity have put emphasis on the modulation of "active" synaptic players. However, synaptic structures that provide the stable framework for synaptic physiology are now beginning to be appreciated as important players in the regulation of synaptic function. Especially, modulating the environment of the synaptic cleft, where the neurotransmitter is released, is likely to be a highly effective strategy to regulate the strength of synaptic transmission. For example, a subtle change in the distance between pre- and postsynaptic membranes, or a change in molecular density within the synaptic cleft would affect the diffusion rate of transmitters. Also, a change in the area-size of the synaptic apposition zone may cause an alteration of transmission efficiency. In fact, synaptic stimulation causes an enlargement of the synaptic apposition zone to such an extent that the change is readily detectable by electron microscopy (Buchs and Muller, 1996). Most intriguingly, synaptic activity induces the widening of the spine head, which are accompanied by flattening of the presynaptic terminal (Colicos et al., 2001). However, the mechanism of how synapses undergo such remodeling has remained elusive.

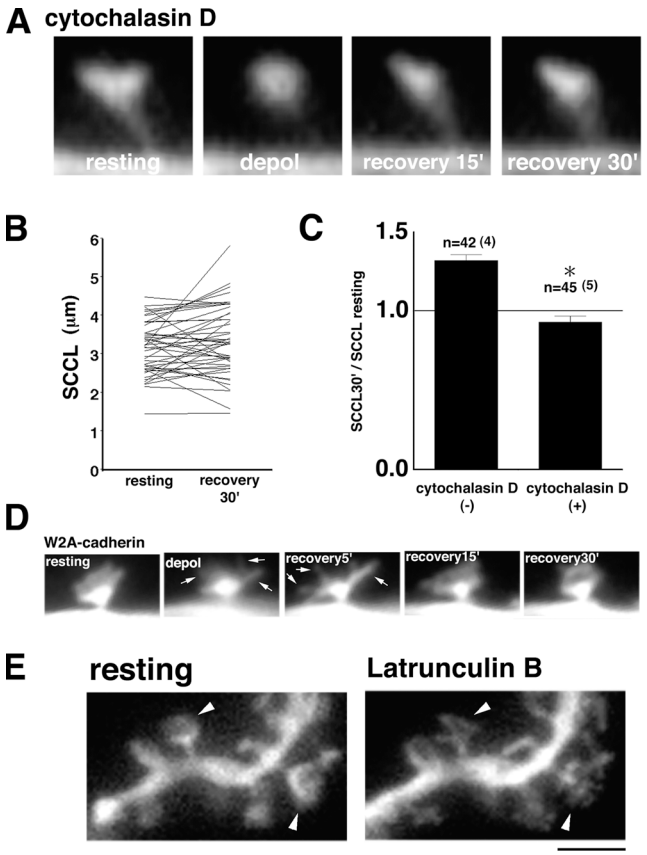

Figure 8. **Involvement of cadherin/actin complex in the rearrangement and the maintenance of spine structure.** (A–C) The activity-induced spine expansion is dependent on actin polymerization. Cytochalasin D was applied 30 min before and during imaging (A). The transient rounding up of spines during the depolarization was not affected by cytochalasin D treatment (A, depol). The spine expansion during the recovery phase was inhibited by cytochalasin D treatment (A, recovery 15′–30′). The SCCL of each spine before and 30 min after depolarization is plotted (B). The ratios between resting SCCL and stimulated (30 min) SCCL are shown (C; mean ± SEM). *$P < 0.05$ to the control. The data were collected from four to five neurons (dendrites) in four to five independent experiments. (D) During (depol) and after the depolarization (recovery 5′), the *W2A-cadherin* transfected neurons protruded filopodia-like structures on the top of the spines (arrows). These protrusions then fuse with each other and retract while moving in various directions (recovery 30′). (E) The neuron was preincubated (30 min) and imaged with existence of latrunculin B. Note that filopodia-like structures formed on the spine top (arrowheads). Bar: (A) 1.47 μm; (D) 2.35 μm; (E) 2.50 μm.

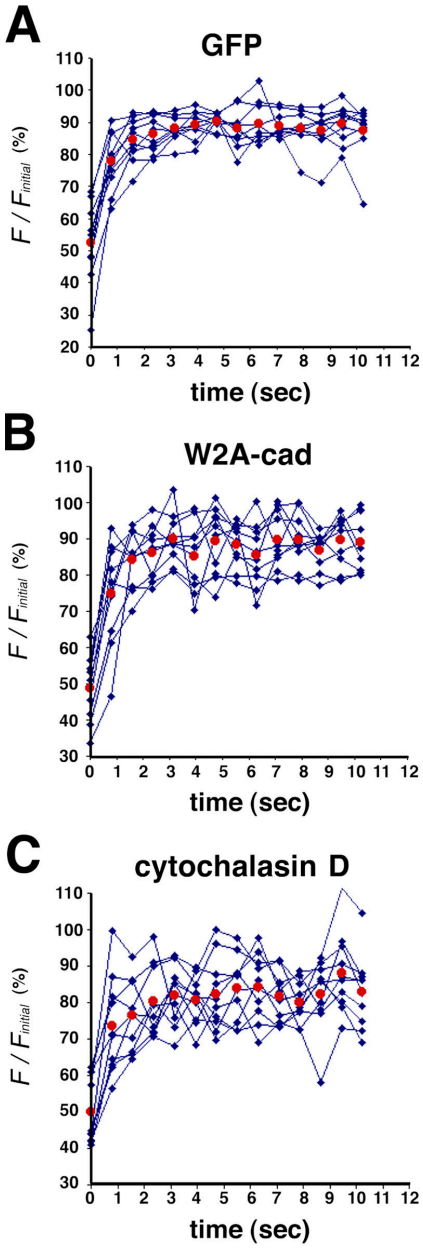

Figure 9. **FRAP analysis to measure the mobility of soluble GFP in spine.** Neurons were transfected with GFP+mock (A and C) or GFP+W2A-cadherin (B) and subjected to FRAP analyses. Cytochalasin D was applied 30 min before FRAP (C). Spines were imaged over time with 788-ms intervals. Circles (red) represent means, diamonds (blue) indicate individual data sets. $F/F_{initial}$, total fluorescence divided by the initial fluorescence.

In this work, insight is provided into the mechanism of how excitatory synapses consisting of glutamatergic terminals and dendritic spines undergo enlargement of the synaptic apposition zone. We propose a model comprising several steps. First, synaptic stimulation that involves AMPA receptor–mediated signaling pathways activates the vigorous rearrangement of actin-cytoskeleton, the putative key regulator of spine morphology (Fischer et al., 2000; Colicos et al., 2001; Furuyashiki et al., 2002). Second, the enriched actin-cytoskeleton may link with its surface counterpart, the cadherins, and become stabilized. Consistent with this idea, there is evidence that β-catenin, a molecular bridge between the actin-cytoskeleton and cadherin, is recruited to the activated spines and coupled with synaptic N-cadherin (Murase et al., 2002), which also becomes stabilized (Tanaka et al., 2000). Third, the synaptic cadherins recruited at the tip of the newly assembled cytoskeleton establish stable cell–cell contacts, if the cadherins find their homophilic partner across the synaptic cleft.

The overexpression of adhesion-defective cadherin mutants, W2A-cadherin and NcadΔE, on the plasma membrane disconnects the linkage between cadherin and the actin-cytoskeleton. In this condition, the actin under remodeling loses its anchor to the cell surface, and in turn, to the adhesive interactions with another cell. Thus, the actin-cytoskeleton under vigorous rearrangement loses its control, protruding random-

shaped structures ad libitum (Fig. 8 D), and yet the changes do not persist without the storage of a "structural memory" in the synaptic adhesive structure.

The activity-induced protrusion on the top of the spines of W2A-cadherin overexpressing neurons (Fig. 8) is reminiscent of the activity-induced development of filopodia (Maletic-Savatic et al., 1999; Ostroff et al., 2002). A small subpopulation of these activity-induced dendritic filopodia establish synaptic contacts with axon terminals and develop mature spines with synaptic markers, such as PSD-95 (Prange and Murphy, 2001). However, many of those which do not establish contact with the presynaptic membranes are likely to be unstable and will retract (Ostroff et al., 2002). Together, with our experiments with W2A-cadherin, both the remodeling of existing synapses and synaptogenesis stimulated by activity persists when these structures establish adhesive contact with the presynaptic membrane. The adhesion molecules on such potential synaptic contacts might be sensors that transmit the extracellular cue to the intracellular machinery that shape synaptic structure.

Long-term effect of the breakage of cadherin-actin linkage

Cultured hippocampal neurons exhibit spontaneous activity (Bekkers and Stevens, 1989). The spontaneous synaptic activity may repetitively stimulate each synaptic junction to enlarge its adhesive area. The disconnection of cadherin-based adhesion from the actin-cytoskeleton should also inhibit these spontaneous forces for synapses to expand the adhesive area (Fig. 7). Probably because of the chronic effect of W2A-cadherin overexpression, the width of each spine becomes smaller. As a result, neurons transfected with *W2A-cadherin* or *NcadΔE* sprouted less numbers of normal spines but more numbers of filopodia, whereas the total numbers of the dendritic protrusions remained the same (Tables I and II). Consistent with this speculation, Togashi and colleagues (Togashi et al., 2002) have demonstrated that a dominant negative cadherin, which has a similar function to W2A-cadherin and NcadΔE, yields narrow-headed, filopodia-like spines. Thus, the apparent developmental effect derived from the chronic manipulation of the cadherin-actin complex seems to be the summation of the results of repetitive synaptic events.

Possible involvement of multiple classical cadherins in the remodeling of synaptic junctions

Various classical cadherin members, such as N- and R-cadherins, cadherin-6, cadherin-8, and cadherin-11 are expressed in CNS (Benson and Tanaka, 1998; Manabe et al., 2000; Tanaka et al., 2000). At least some of them are localized in synaptic membranes. There is the observation that there are some synapses which express β-catenin, but without N-cadherin; it is possible that these synapses may express other classical cadherins (Benson and Tanaka, 1998). Certain classical cadherins may label a certain population of N-cadherin-negative synapses, and some other classical cadherin members may colabel a subpopulation of N-cadherin–labeled synapses in combination.

Expression of the W2A-cadherin or NcadΔE probably modulates cadherin-based synaptic adhesion by competing with the intrinsic cadherin–catenin interaction. Also, it is probable that in some synapses W2A-cadherin may inhibit the adhesiveness of other classical cadherins, because these classical cadherins share common cytoplasmic binding sites for catenins, and in turn, the actin-cytoskeleton. Therefore, W2A-cadherin overexpression may yield an overall suppression of the sum of the adhesiveness by various classical cadherins. However, concerning the excitatory synapses that are established on the top of the dendritic spines of hippocampal neurons, all the synapses are highly positive for N-cadherin (Benson and Tanaka, 1998). Moreover, N-cadherin, but not R-cadherin, cadherin-6, or cadherin-8, exhibits activity-induced dimerization and the acquirement of trypsin-resistance (Tanaka et al., 2000). Therefore, it is likely that the phenomena resulting from W2A-cadherin overexpression may largely reflect the dysfunction of N-cadherin.

Conclusion

This work shows a significance of the linkage of the cell adhesion molecules resides in the pre- and postsynaptic membranes with actin-cytoskeleton during the remodeling process of the synaptic junction. This work, as well as previous studies (Fischer et al., 2000; Colicos et al., 2001), indicates that synaptic activity triggers active remodeling of the synaptic cytoskeleton that involves actin-polymerization. This driving force for the cyto-architectural rearrangement is organized and stabilized by its linkage to cadherins, which recognizes the partner cell membrane with which to form synapse. Synaptic cadherin might be a sensor that transmits the environmental information across the synaptic cleft to the cytoskeleton under active rearrangement in synaptic cytoplasm.

Materials and methods

Neuron culture and transfection

Hippocampal neurons were cultured from E18 rat embryos as described previously (Banker and Goslin, 1991) with modifications. Neurons were plated at a density of 0.9–1.0 $\times$ 10^4 cells/cm^2 onto poly-L-lysine–coated glass-bottomed dish (Matsunami, Ltd.). Neurons were supplied with Neurobasal/B27 without the addition of AraC after the routine dissection. On day 6, the medium was replaced with fresh Neurobasal/B27 with the addition of APV (100 μM; Sigma-Aldrich), whereas the conditioned medium was kept in the CO_2 incubator. The mixtures of expression vectors were prepared to adjust the total DNA content to 4 μg per dish. For example, 3.0 μg of *N-cadherin-myc* vector was mixed with 1.0 μg of *gfp* vector to obtain adequate expression levels of the both proteins. The cDNA mixture was diluted with 60 μl of 0.25 M $CaCl_2$, and then with 60 μl of 2×BES buffered saline (280 mM NaCl, 1.5 mM Na_2HPO_4, 50 mM BES, pH 7.1). The mixture was immediately dropped onto the dish and incubated for 45 min in 5% CO_2 atmosphere at 37°C. After checking the formation of fine $CaPO_4$–DNA complex, the neurons were washed twice with Hepes-buffered saline (20 mM Hepes-NaOH, pH 7.4, 135 mM NaCl, 4 mM KCl, 1 mM Na_2HPO_4, 2 mM $CaCl_2$, 10 mM glucose), refed with the conditioned medium, and further cultured until the neurons were analyzed. Distributions of the intrinsic/heterologous proteins were visualized by immunostaining (Tanaka et al., 2000) with anti–N-cadherin (a gift from G. Phillips, Mt. Sinai School of Medicine, New York, NY; Phillips et al., 2001), anti-synaptophysin (rabbit; Zymed Laboratories), anti–PSD-95 (mouse; Upstate Biotechnology), anti-GFP (rabbit; Molecular Probe), and anti–c-myc (mouse; Calbiochem) antibodies.

Time-lapse imaging

Neurons transfected with *gfp* or *N-cadherin-venus* cDNAs were cultured until 18 DIV. After changing the culture medium to Tyrode solution (25 mM Hepes-NaOH, 119 mM NaCl, 2.5 mM KCl, 2.0 mM $CaCl_2$, 2.0 mM $MgCl_2$, pH 7.4), the culture dish was mounted in a chamber at 37°C for

live recording. For high K^+-stimulation, 1.5 ml of Tyrode-HK solution (25 mM Hepes-NaOH, 71.5 mM NaCl, 50 mM KCl, 2.0 mM $CaCl_2$, 2.0 mM $MgCl_2$, pH 7.4) was added to the culture dish filled with 1 ml of normal Tyrode making the final $[K^+]$ at 31 mM.

Microscopes and measurements

CCD images were obtained on a microscope (model Eclipse TE100; Nikon) equipped with GFP-optimized filter set (model MBE34931;Nikon) and CCD camera (model C4742-95; Hamamatsu). A 60× 1.40 NA oil-immersion objective (PlanApo; Nikon) was used to project images to the camera without an intermediate projection lens. Luminavision software (Mitani) was used to control mechanical shutters and filter wheels. Measurements of the projected images were performed with MacSCOPE software (Mitani). Optical section images of sixty focal planes 0.2 μm apart were collected by the use of a DeltaVision deconvolution microscope system (Applied Precision, Inc.) as described previously (Haraguchi et al., 1999). Images of spines resulted in a nominal spatial resolution of 0.11 μm/pixel by the use of a 60× 1.40 NA oil immersion objective (PlanApo; Olympus). Deconvolution of the collected data were performed as described previously (Agard et al., 1989). Confocal time-lapse imaging was performed by the use of a heating chamber (IN-ONI-F2; Tokai Hit) combined with a confocal microscope system (Radiance 2100; Bio-Rad Laboratories) assisted by LaserSharp software (Bio-Rad Laboratories). A 60× 1.40 NA oil immersion objective was used (PlanApo; Nikon). Images of spines were acquired at the 3× digital zoom, resulting in a nominal spatial resolution of 0.13 μm/pixel and in a time resolution of 39 μs/point in frame-scan mode. For each imaged spine, a *z*-stack at intervals of 0.2 μm was taken to allow the reconstruction of spine morphology. Measurements of signal intensity and dimensions were performed by using LaserPix software (Bio-Rad Laboratories).

The thickest main dendrite in each neuron was subjected to the analyses. For the measurement of the dimensions of spines, the spines on the 10-μm-long dendritic segment between 30 and 40 μm from the proximal origin were analyzed. About eight to nine protrusions, including spines and nonspine protrusions, were found on the 10-μm-long segment. Among these protrusions, data were collected from all the spines visualized in the same focal plane. For the counting of the type of the dendritic protrusions, and in the analyses with confocal microscopy, the dendritic segment between 20 and 40 μm from the proximal origin was analyzed. At least four independent experiments were performed to obtain more than four different neurons subjected to data collection. Capturing image and measuring spine dimension were performed blind by independent researchers. Values are shown as mean ± SEM.

FRAP experiments

FRAP experiments were performed by the use of a confocal microscope (model LSM510; Carl Zeiss MicroImaging, Inc.) equipped with a 63×, 1.40 NA oil immersion objective (Plan-Apochromat; Carl Zeiss MicroImaging, Inc.) as described previously (Richards et al., 2004). The whole area of the spine of interest was defined as the region of interest, and bleached with 100% laser intensity for 1.5 s. Recovery was measured by rapid imaging of a single image plane of 256 × 256 $pixels^2$ size, with the 3× digital zoom, resulting in a nominal spatial resolution of 0.19 μm/pixel and in a time resolution of 1.76 μs/point in frame-scan mode. Two trials were performed per spine and averaged.

Quantification of the size of synaptic puncta

Each coverslip was scanned from one end to another, and every neuron was serially photographed with a 40× objective. The first five neurons from one end of the coverslip were counted. Each photograph was taken by 1,000 ms of exposure, and the labeled area was extracted with a threshold of signal intensity at the level of 100 among 0–255. Puncta on the proximal 50 μm segment of the thickest dendrite of each neuron were measured. Huge areas >3 μm^2 were excluded from the measurement because those were supposed to be the fused area consisted of multiple puncta. The counting was performed with four coverslips from independent preparations. Photographing and counting were performed blind by independent investigators. The data were compared by unpaired *t* test.

Construction of plasmid vectors

Expression vectors for *N-cadherin* mutants were constructed by modifying *pCXN2-Ncad-myc*, in which *N-cadherin* fused with *6xmyc*-tag is ligated downstream of β-*actin* promoter (a gift from W. Shan, Montreal Neurological Institute; Shan et al., 2000). The NH_2-terminal region of *N-cadherin* between EcoRI and KpnI sites was replaced with the corresponding fragment derived from the W2A-cadherin (a gift from K. Tamura, Hyogo Medical School, Kobe, Japan; Tamura et al., 1998). *N-cadherin-venus* was constructed by replacing the *6xmyc* region (between XhoI and BglII sites) of *pCXN2-Ncad-myc* with *venus* (a gift from A. Miyawaki, RIKEN, Wako, Japan; Nagai et al., 2002) amplified by PCR. The integrity of the vectors was verified by DNA sequencing.

Cell aggregation assay

N-cadherin-myc was stably transfected to L929 cells by Neomycin selection. The double transfectant cells were obtained by transfecting *W2A-cadherin-flag* vector possessing Zeocin resistant cassette to *N-cadherin-myc* stable transfectant and selected with 100 μg/ml Zeocin. A Zeocin-resistant *W2A-cadherin-flag* expression vector was constructed by ligating a blunt-ended *ZEO*-cassette (*pCMV/Zeo*, cut with EcoRV and PvuII; Invitrogen) into the StuI site, a W2A-cadherin between the EcoRI and XhoI sites and a flag between XhoI and BglII sites of pCXN2, respectively. Cell aggregation assay was performed as described previously (Takeichi, 1977).

We thank Shigeo Okabe, Yasushi Sako, Toshio Yanagida, and Haruo Kasai for advice in microscopy; Greg Phillips, Weisong Shan, Kazuyoshi Tamura, and Atsushi Miyawaki for reagents; and Hong Shi for technical assistance.

This work was supported by Grant-in-Aid for Scientific Research on Priority Area [C]-Advanced Brain Science Project from Ministry of Education, Culture, Sports, Science and Technology, Japan (to H. Tanaka), and NS20147 from National Institutes of Health (to D.R. Colman). K. Okamura was supported by Iwadare Association for Dental Graduate Students.

Submitted: 4 June 2004
Accepted: 28 October 2004

References

Abe, K., O. Chisaka, F. Van Roy, and M. Takeichi. 2004. Stability of dendritic spines and synaptic contacts is controlled by alphaN-catenin. *Nat. Neurosci.* 7:357–363.

Agard, D.A., Y. Hiraoka, P. Shaw, and J.W. Sedat. 1989. Fluorescence microscopy in three dimensions. *Methods Cell Biol.* 30:353–377.

Bamji, S.X., K. Shimazu, N. Kimes, J. Huelsken, W. Birchmeier, B. Lu, and L.F. Reichardt. 2003. Role of beta-catenin in synaptic vesicle localization and presynaptic assembly. *Neuron.* 40:719–731.

Banker, G., and K. Goslin. 1991. Culturing nerve cells. The MIT Press, London. 453 pp.

Bekkers, J.M., and C.F. Stevens. 1989. NMDA and non-NMDA receptors are co-localized at individual excitatory synapses in cultured rat hippocampus. *Nature.* 341:230–233.

Benson, D.L., and H. Tanaka. 1998. N-cadherin redistribution during synaptogenesis in hippocampal neurons. *J. Neurosci.* 18:6892–6904.

Bozdagi, O., W. Shan, H. Tanaka, D.L. Benson, and G.W. Huntley. 2000. Increasing numbers of synaptic puncta during late-phase LTP: N-cadherin is synthesized, recruited to synaptic sites, and required for potentiation. *Neuron.* 28:245–259.

Buchs, P.A., and D. Muller. 1996. Induction of long-term potentiation is associated with major ultrastructural changes of activated synapses. *Proc. Natl. Acad. Sci. USA.* 93:8040–8045.

Colicos, M.A., B.E. Collins, M.J. Sailor, and Y. Goda. 2001. Remodeling of synaptic actin induced by photoconductive stimulation. *Cell.* 107:605–616.

Fannon, A.M., and D.R. Colman. 1996. A model for central synaptic junctional complex formation based on the differential adhesive specificities of the cadherins. *Neuron.* 17:423–434.

Fischer, M., S. Kaech, D. Knutti, and A. Matus. 1998. Rapid actin-based plasticity in dendritic spines. *Neuron.* 20:847–854.

Fischer, M., S. Kaech, U. Wagner, H. Brinkhaus, and A. Matus. 2000. Glutamate receptors regulate actin-based plasticity in dendritic spines. *Nat. Neurosci.* 3:887–894.

Furuyashiki, T., Y. Arakawa, S. Takemoto-Kimura, H. Bito, and S. Narumiya. 2002. Multiple spatiotemporal modes of actin reorganization by NMDA receptors and voltage-gated Ca^{2+} channels. *Proc. Natl. Acad. Sci. USA.* 99:14458–14463.

Geinisman, Y., L. deToledo-Morrell, and F. Morrell. 1991. Induction of long-term potentiation is associated with an increase in the number of axospinous synapses with segmented postsynaptic densities. *Brain Res.* 566: 77–88.

Gumbiner, B.M., and P.D. McCrea. 1993. Catenins as mediators of the cytoplasmic functions of cadherins. *J. Cell Sci. Suppl.* 17:155–158.

Haraguchi, T., D.Q. Ding, A. Yamamoto, T. Kaneda, T. Koujin, and Y. Hiraoka. 1999. Multiple-color fluorescence imaging of chromosomes

and microtubules in living cells. *Cell Struct. Funct.* 24:291–298.

Hosokawa, T., M. Ohta, T. Saito, and A. Fine. 2003. Imaging spatio-temporal patterns of long-term potentiation in mouse hippocampus. *Philos. Trans. R. Soc. Lond. B Biol. Sci.* 358:689–693.

Inoue, T., T. Tanaka, S.C. Suzuki, and M. Takeichi. 1998. Cadherin-6 in the developing mouse brain: expression along restricted connection systems and synaptic localization suggest a potential role in neuronal circuitry. *Dev. Dyn.* 211:338–351.

Kintner, C. 1992. Regulation of embryonic cell adhesion by the cadherin cytoplasmic domain. *Cell.* 69:225–236.

Korkotian, E., and M. Segal. 1999. Release of calcium from stores alters the morphology of dendritic spines in cultured hippocampal neurons. *Proc. Natl. Acad. Sci. USA.* 96:12068–12072.

Majewska, A., A. Tashiro, and R. Yuste. 2000. Regulation of spine calcium dynamics by rapid spine motility. *J. Neurosci.* 20:8262–8268.

Maletic-Savatic, M., R. Malinow, and K. Svoboda. 1999. Rapid dendritic morphogenesis in CA1 hippocampal dendrites induced by synaptic activity. *Science.* 283:1923–1927.

Manabe, T., H. Togashi, N. Uchida, S.C. Suzuki, Y. Hayakawa, M. Yamamoto, H. Yoda, T. Miyakawa, M. Takeichi, and O. Chisaka. 2000. Loss of cadherin-11 adhesion receptor enhances plastic changes in hippocampal synapses and modifies behavioral responses. *Mol. Cell. Neurosci.* 15: 534–546.

Matsuzaki, M., N. Honkura, G.C. Ellis-Davies, and H. Kasai. 2004. Structural basis of long-term potentiation in single dendritic spines. *Nature.* 429: 761–766.

Miskevich, F., Y. Zhu, B. Ranscht, and J.R. Sanes. 1998. Expression of multiple cadherins and catenins in the chick optic tectum. *Mol. Cell. Neurosci.* 12: 240–255.

Murase, S., E. Mosser, and E.M. Schuman. 2002. Depolarization drives beta-catenin into neuronal spines promoting changes in synaptic structure and function. *Neuron.* 35:91–105.

Nagai, T., K. Ibata, E.S. Park, M. Kubota, K. Mikoshiba, and A. Miyawaki. 2002. A variant of yellow fluorescent protein with fast and efficient maturation for cell-biological applications. *Nat. Biotechnol.* 20:87–90.

Ostroff, L.E., J.C. Fiala, B. Allwardt, and K.M. Harris. 2002. Polyribosomes redistribute from dendritic shafts into spines with enlarged synapses during LTP in developing rat hippocampal slices. *Neuron.* 35:535–545.

Phillips, G.R., J.K. Huang, Y. Wang, H. Tanaka, L. Shapiro, W. Zhang, W.S. Shan, K. Arndt, M. Frank, R.E. Gordon, et al. 2001. The presynaptic particle web: ultrastructure, composition, dissolution, and reconstitution. *Neuron.* 32:63–77.

Prange, O., and T.H. Murphy. 2001. Modular transport of postsynaptic density-95 clusters and association with stable spine precursors during early development of cortical neurons. *J. Neurosci.* 21:9325–9333.

Richards, D.A., V. De Paola, P. Caroni, B.H. Gahwiler, and R.A. McKinney. 2004. AMPA-receptor activation regulates the diffusion of a membrane marker in parallel with dendritic spine motility in the mouse hippocampus. *J. Physiol.* 558:503–512.

Shan, W.S., H. Tanaka, G.R. Phillips, K. Arndt, M. Yoshida, D.R. Colman, and L. Shapiro. 2000. Functional cis-heterodimers of N- and R-cadherins. *J. Cell Biol.* 148:579–590.

Takeichi, M. 1977. Functional correlation between cell adhesive properties and some cell surface proteins. *J. Cell Biol.* 75:464–474.

Takeichi, M. 1990. Cadherins: a molecular family important in selective cell-cell adhesion. *Annu. Rev. Biochem.* 59:237–252.

Tamura, K., W.S. Shan, W.A. Hendrickson, D.R. Colman, and L. Shapiro. 1998. Structure-function analysis of cell adhesion by neural (N-) cadherin. *Neuron.* 20:1153–1163.

Tanaka, H., W. Shan, G.R. Phillips, K. Arndt, O. Bozdagi, L. Shapiro, G.W. Huntley, D.L. Benson, and D.R. Colman. 2000. Molecular modification of N-cadherin in response to synaptic activity. *Neuron.* 25:93–107.

Tang, L., C.P. Hung, and E.M. Schuman. 1998. A role for the cadherin family of cell adhesion molecules in hippocampal long-term potentiation. *Neuron.* 20:1165–1175.

Togashi, H., K. Abe, A. Mizoguchi, K. Takaoka, O. Chisaka, and M. Takeichi. 2002. Cadherin regulates dendritic spine morphogenesis. *Neuron.* 35: 77–89.

Toni, N., P.A. Buchs, I. Nikonenko, C.R. Bron, and D. Muller. 1999. LTP promotes formation of multiple spine synapses between a single axon terminal and a dendrite. *Nature.* 402:421–425.

Uchida, N., Y. Honjo, K.R. Johnson, M.J. Wheelock, and M. Takeichi. 1996. The catenin/cadherin adhesion system is localized in synaptic junctions bordering transmitter release zones. *J. Cell Biol.* 135:767–779.

Yamagata, K., K.I. Andreasson, H. Sugiura, E. Maru, M. Dominique, Y. Irie, N. Miki, Y. Hayashi, M. Yoshioka, K. Kaneko, et al. 1999. Arcadlin is a neural activity-regulated cadherin involved in long term potentiation. *J. Biol. Chem.* 274:19473–19479.

Yamagata, M., J.P. Herman, and J.R. Sanes. 1995. Lamina-specific expression of adhesion molecules in developing chick optic tectum. *J. Neurosci.* 15: 4556–4571.

Zhang, W., and D.L. Benson. 2001. Stages of synapse development defined by dependence on F-actin. *J. Neurosci.* 21:5169–5181.